引用格式：MA Lilong, XIE Minchao, OU Wei, et al. Fabrication and Lasing Properties of Silicon-based GaN Microcavities (Invited)[J]. Acta Photonica Sinica, 2022, 51(2):0251204
马立龙,谢敏超,欧伟,等.硅基GaN微腔制作及其激射特性(特邀)[J].光子学报,2022,51(2):0251204

硅基GaN微腔制作及其激射特性(特邀)

马立龙,谢敏超,欧伟,梅洋,张保平
(厦门大学 电子科学与技术学院 微纳光电子研究室,福建 厦门 361005)

摘　要:提出了一种新的Si衬底上GaN微盘谐振腔的制备方式,避免了传统Si基GaN器件中晶体质量较差以及外延层较厚对器件性能的影响。本工作中GaN的外延生长使用蓝宝石衬底,随后将外延层转移至硅衬底上进行微盘谐振腔的制备。外延生长时靠近衬底侧的GaN富缺陷层可使用减薄抛光的方式去除,并且通过简单湿法刻蚀二氧化硅牺牲层即可实现GaN微盘与Si衬底之间的空气间隙结构。基于较好的晶体质量与低损耗的谐振腔,实现了高Q值的Si基GaN微盘谐振腔低阈值激射,阈值能量低至5.2 nJ/pulse,Q值最高为10 487。同时,器件具有较好的温度稳定特性,在100 ℃环境下也能维持低阈值激射,为大规模单片硅基光子集成提供了高性能的激光源。

关键词:半导体器件与技术;微腔;氮化镓;硅;高品质因子;低阈值;高温工作
中图分类号:TN365　　**文献标识码**:A　　**doi**:10.3788/gzxb20225102.0251204

0　引言

半导体微谐振腔能将有源介质所发出的光子限制在与光波长可比拟的一个小体积范围内,进而展现出许多新颖的物理光学特性。使用半导体微谐振腔可以人为地调控谐振腔内有源介质的自发辐射特性,以开发更为高效的光电子器件。同时,半导体微谐振腔也是进行腔量子电动力学(Cavity Quantum Electrodynamics, CQED)等基础研究的一个极好的平台[1-2]。基于半导体微腔的光电子器件如今已得到广泛应用,如半导体微腔激光器、微腔传感器、微腔光过滤器等。具有代表性的半导体光学微腔结构主要有三种,分别为法布里一珀罗(Fabry-Pérot, FP)型微腔、光子晶体(Photonic Ciystal, PC)型微腔和回音壁模式(Wispering-Gallery Mode, WGM)微腔[3]。其中,在WGM半导体微腔中,光子沿半导体波导层侧壁循环传播,通过在波导层与周围空气界面处发生的全反射来形成对光场的限制,因此WGM微腔能够实现极高的Q值与较小的模式体积。而且WGM微腔相比于前两种微腔结构简单、制备方便,且更加易于片上集成,在光电子集成领域具有十分重要的应用。

GaN基半导体材料是一种具有直接带隙的宽禁带半导体材料,包括AlN、GaN、InN以及他们之间的多元合金。通过调整合金组分,其发光波长可以覆盖深紫外至近红外波段,因此是制备光电子器件极为重要的半导体材料[4-7]。此外,GaN基半导体材料具有较大的激子束缚能以及振子强度,与WGM微腔结合可实现小体积、高效率的微腔光电子器件,且可用于室温下腔量子电动力学研究[8-9]。因此,GaN基WGM微腔发光器件一直吸引着众多研究者的注意,已经在光电集成、光谱分析[10]、生物医学诊断[11]、强耦合腔量子电动力学[6,12-13]等领域中得到了广泛的应用。

自20世纪80年代中后期日本学者研制出蓝紫光波段的GaN基发光二极管和激光器以来[14],GaN基微腔激光器快速发展。而将GaN微腔激光器与Si衬底结合可以大幅度降低制造成本,并且在大规模低成本硅

基金项目:国家重点研究发展计划(No. 2017YFE0131500),国家自然科学基金(No. 62104204),厦门大学校长基金(No. ZK1029)
第一作者:马立龙(1999－),女,硕士研究生,主要研究方向为宽禁带半导体器件。Email: malilong1@stu.xmu.edu.cn
导师(通讯作者):梅洋(1994－),男,讲师,博士,主要研究方向为宽禁带半导体材料与器件。Email: meiyang@ xmu.edu.cn
张保平(1963－),男,教授,博士,主要研究方向为宽禁带半导体材料与器件。Email: bzhang@ xmu.edu.cn
收稿日期:2021-11-01;**录用日期**:2021-12-26

光子集成领域有着愈发重要的应用价值，因此受到了广泛的关注。对于早期FP型GaN基激光器而言，随着研究人员对FP型激光器高性能的不断追求，其室温下激射阈值不断降低。2011年，名古屋大学的AMANO H研究组报道了生长于Si衬底上InGaN量子阱结构的受激辐射[15]。2015年，通过改善晶体质量并且使用脊形结构，他们将受激辐射阈值进一步降低至6 MW/cm^2[16]。2019年，来自中山大学的ZHANG B的研究小组也报道了Si衬底上使用选区外延法生长的多量子阱激光器，在室温条件下实现了433 nm的光泵浦激射，阈值为1.85 MW/cm^2[17]。以上结果均为光泵浦下实现。2016年，中科院苏州纳米所的研究小组实现了第一支室温下电注入Si基GaN激光器，激射波长413 nm，阈值电流密度4.7 kA/cm^2[18]；随后通过进一步改善有源区晶体质量、提升内量子效率，将器件激射阈值电流进一步降低至2.25 kA/cm^2[19]；2018年，通过降低刃位错密度，他们实现了UVA波段的Si基GaN激光器的室温电注入激射，工作波长为389 nm[20]。

GaN基WGM微腔激光器相比传统的FP型激光器具有更小的模式体积、更低的阈值和损耗。2006年，加利福尼亚大学HU E L课题组报告了第一个室温下的Si基GaN微盘光泵浦激光器，在低阈值方面显示出了巨大的潜力[21]。2014年，CHOI H W等通过微球光刻、干湿蚀刻等工艺，制造了含有InGaN/GaN多量子阱的Si基GaN微盘，在室温光泵浦下实现了438 nm的激射[22]。2017年，南京邮电大学ZHU G Y等报道了在光泵浦下的单模紫外GaN基WGM微腔激光器[23]。对于电注入器件，2018年，中科院苏州纳米所的研究小组提出了“三明治”结构的Si基GaN微盘激光器，实现了室温电泵浦脉冲激射[24]。2020年，该课题组通过降低p-AlGaN包层的碳杂质浓度，首次实现了连续波电注入下的激射[25]。目前基于Si衬底上GaN微盘谐振腔的激光器、传感器等已有较多研究，激光器的激射波长也已覆盖深紫外至绿光波段[26-29]。

然而，高质量Si基GaN微盘谐振腔也面临着许多困难，包括Si与GaN之间的晶格失配、热膨胀系数失配、以及外延生长过程中的回融刻蚀[30]等。GaN和Si之间存在着17%的晶格失配，因此在外延生长时会引起高密度穿透位错（通常为10^{10} cm^{-2}）。这不仅会降低有源区的内量子效率，还会造成顶部和底部薄膜的界面粗糙，增加谐振腔的散射损耗。另一方面，GaN与硅衬底之间存在54%的热膨胀系数失配，在外延生长后降温过程中会导致GaN薄膜中出现较大的拉伸应力，使得晶片发生翘曲甚至龟裂[31-32]。因此，为了保证有源区的质量，往往需要预生长比较厚的应力调整与缺陷过滤层[33-34]。而且，外延生长所使用的Ga源也会腐蚀Si衬底，即回融刻蚀，因此在生长GaN之前通常需要生长一定厚度的AlN缓冲层以保护Si衬底[35]。以上原因会使得Si衬底上GaN外延层厚度较大（一般大于1 μm），制成微盘谐振腔较厚，难以保证单模工作，降低了谐振腔的光限制能力以及微腔效应。另外，在靠近衬底的氮化物薄膜中往往具有高密度的缺陷与位错，其内部光学吸收与散射损耗较大，同样会影响微腔的品质因子（Q值）和微盘激光器的阈值。PUCHTLER T等的研究证明，构成微盘的材料的位错密度与谐振腔的Q值之间存在直接负相关特性[36]。

为了解决以上Si基GaN微盘谐振腔所面临的问题，本文提出了一种新的器件制备方法，避免了Si衬底上晶体质量较差以及外延层较厚对器件的影响，实现了高Q值的Si基GaN微盘谐振腔低阈值激射。为保证晶体质量，GaN的外延生长采用蓝宝石衬底。在微盘制备过程中将外延层转移至Si衬底上，并将原始生长过程中衬底附近的富缺陷层去除。最后通过简单的二氧化硅牺牲层湿法刻蚀实现GaN微盘与Si衬底之间的空气间隙结构。通过以上方法，成功实现了高质量Si基GaN微盘谐振腔的制备，并在光泵浦条件下实现了低阈值激射。谐振腔Q值高达10 487，为目前可见光波段GaN基微盘谐振腔最高值。器件阈值能量低至5.2 nJ/pulse，对应能量密度为33.6 μJ/cm^2。由于良好的晶体质量以及较低的谐振腔损耗，器件在100 ℃温度下仍能保持优异的激射特性。同时，本文的制备方法具有较好的灵活性，可将GaN基微盘谐振腔制备在任何基板上，如金属、聚合物、石英和半导体等。

1 硅基氮化镓微腔制备

采用金属有机物化学气相沉积技术（Metal-organic Chemical Vapor Deposition，MOCVD）在（0001）面蓝宝石衬底上外延生长GaN基外延层，其结构包括2 μm厚的u-GaN层、2 μm厚的n-GaN层，5对$In_{0.1}Ga_{0.9}N$（3 nm/5 nm）量子阱、20 nm Mg掺杂的p-$Al_{0.2}Ga_{0.8}N$层以及97 nm的p-GaN层。外延片发光中心波长～420 nm，其自发辐射光谱如图1。需要注意的是，以上外延结构同时为电注入谐振腔的制备而设计，因此进行了p型与n型掺杂，在之前的工作中，已经成功制备了电注入GaN基微盘谐振腔[37]。本文中直接使用此外延结构

进行Si基光泵浦GaN微腔的制备。为了将GaN微盘谐振腔制作于Si衬底上，采用了薄膜转移技术，器件制备过程如图2。首先，在晶圆表面沉积约300 nm厚的SiO_2牺牲层（步骤1）。然后将晶片倒装键合在Si衬底上，通过激光剥离的方式（Laser Lift-Off，LLO）去除蓝宝石衬底，激光剥离能量为50 mJ，光斑面积为2.4 mm^2。利用化学机械抛光（Chemical Mechanical Polishing，CMP）去除外延生长时蓝宝石衬底附近的富缺陷层（步骤2和3）。抛光过程中使用碱性抛光液，转盘转速为35 r/min，去除外延层厚度为~3.77 μm。随后，通过感应耦合等离子体（Inductively Coupled Plasma，ICP）刻蚀形成微盘台面，刻蚀截止层为SiO_2层（步骤4）。ICP刻蚀过程中上下电极功率分别为180 W与80 W，刻蚀气体为Ar/Cl_2。最后，通过氢氟酸（HF）溶液湿法蚀刻去除部分SiO_2牺牲层，使得GaN微盘边缘与Si衬底之间形成悬空结构，剩余的SiO_2微柱可对GaN微盘进行支撑，完成器件制备（步骤5）。最终微盘的厚度为~375 nm。扫描电子显微镜（Scanning Electron Microscope，SEM）图像如图3，微盘直径为28 μm。从微盘边缘区域局部SEM放大图中可以清楚地观察到腐蚀SiO_2牺牲层所形成的空气间隙结构以及平坦光滑的微盘侧壁，这对于减小谐振腔散射损耗、增加光场限制能力至关重要。通过高精度减薄与抛光工艺，微盘的厚度减薄至约375 nm，可维持低阶WGM的振荡。

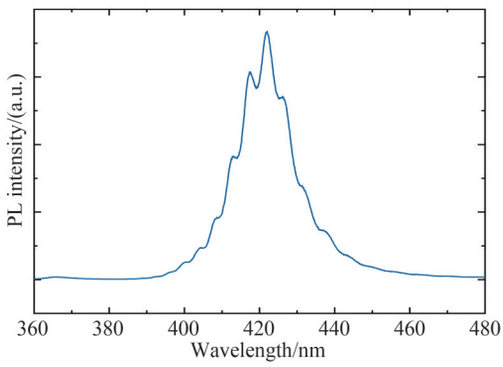

图1　外延片自发辐射光谱

Fig.1　Spontaneous emission spectrum of the epitaxial wafer

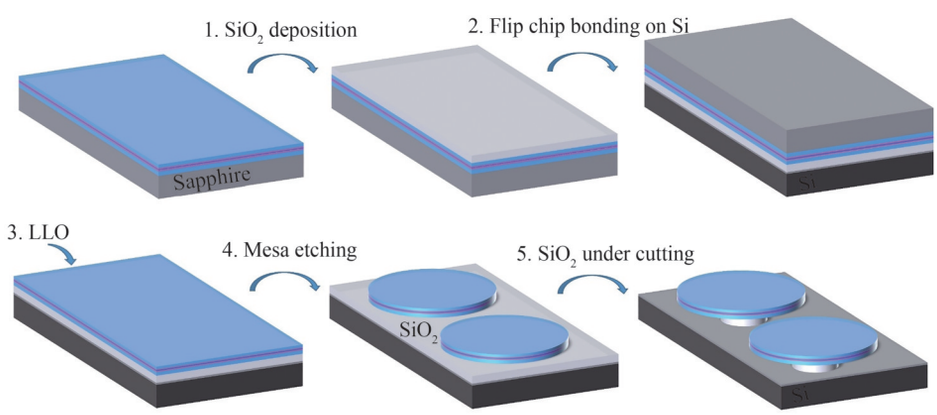

图2　硅基GaN微腔的制备工艺流程

Fig.2　Fabrication processes of the GaN based microcavity on Si

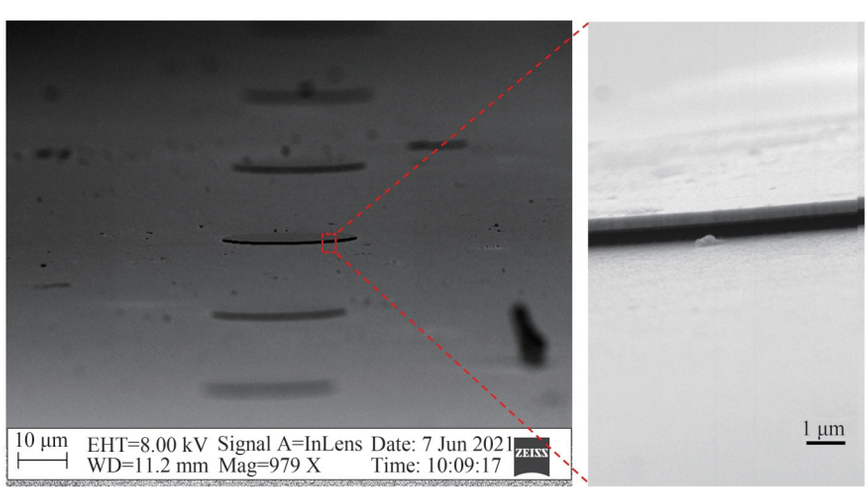

图3　硅基GaN微腔的SEM图

Fig.3　SEM image of GaN based microcavity on Si

2 Si基GaN微腔的激射特性

为了表征Si衬底上GaN基微盘谐振腔的光学特性，使用微区光致发光（Micro-Photoluminescence，μ-PL）系统对样品进行了测试。所使用的激发光源为CryLas-FTSS355-Q1脉冲激光器，发光波长为355 nm，重复频率为15 kHz，脉宽为1 ns。激发光源经由显微镜物镜（NA0.35，40×）聚焦后照射至样品表面，光斑直径约为70 μm。微盘发出的光从其顶部收集，经由相同物镜后通过自由空间光路导入光谱仪。不同激发能量下微盘发光光谱如图4(a)，从图中可以看出，当激发能量为4 nJ/pulse时，微盘显示出量子阱较宽的自发辐射光谱。当激发能量逐渐增加至阈值附近时，在413 nm附近会出现几个尖锐的发光峰，并且其强度迅速增强最终实现激射。图4(b)展示了微盘器件发光强度随激发能量变化曲线，强度的非线性增长表现出了明显的阈值特性，进一步证明了谐振腔内激光的产生。器件阈值激发能量低至5.2 nJ/pulse，对应于的阈值能量密度为33.6 μJ/cm^2，这是Si基GaN微盘激光器中较低的结果[38-39]。图4(c)为GaN微盘在几个特定激发能量下的发光照片。小能量下微盘整体发光，随着激发能量增强至激射阈值附近，微盘边缘处发光更强，当超出阈值后，微盘边缘发光则完全占据主导状态，并且光场被很好地限制在微盘之内。这种发光特性的转变是WGM产生振荡并最终激射的明显特征。本工作中Si基GaN微腔的低阈值激射可归因于高晶体质量、平坦的微盘表面和侧壁。

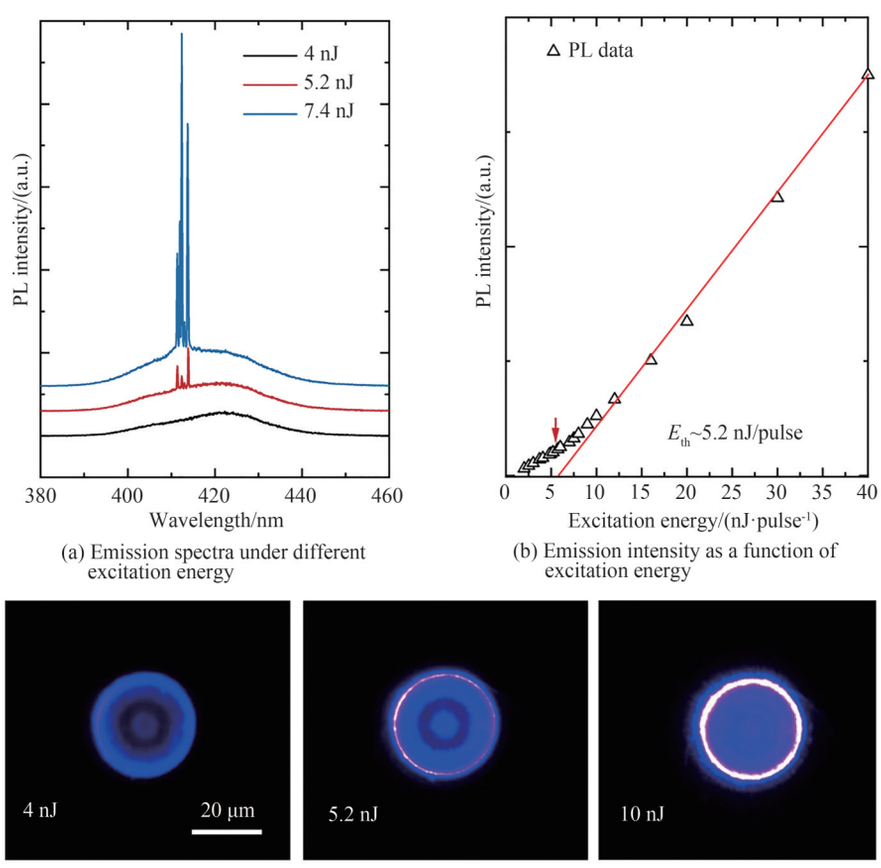

图4 微盘器件激射特性

Fig.4 Lasing characteristics of microdisk devices

从图4(a)中可以看出，在大激发能量下器件光谱出现多个谐振模式，为了进一步研究其模式特性，对器件进行了变激发能量高分辨率光谱测试，不同能量下器件归一化光谱如图5(a)。在小激发能量下，器件表现出单模激射特性，只在413.2 nm处出现一个发光峰。随着激发能量增大，短波长处出现更多高阶的WGM，且出现明显模式竞争效应，更短波长处模式发光强度随激发能量增加不断增强。这主要是由于量子阱有源区的增益谱随激发能量增加而蓝移所致。本文也测试了微盘激光器的偏振特性，如图5(b)。器件发

光偏振度计算表达式为

$$P=\frac{I_{\_max}-I_{\_min}}{I_{\_max}+I_{\_min}} \tag{1}$$

式中，$I_{_max}$与$I_{_min}$分别为不同偏振角下器件发光强度的最大与最小值。激射后器件展示出良好的偏振特性，偏振度约为70%。

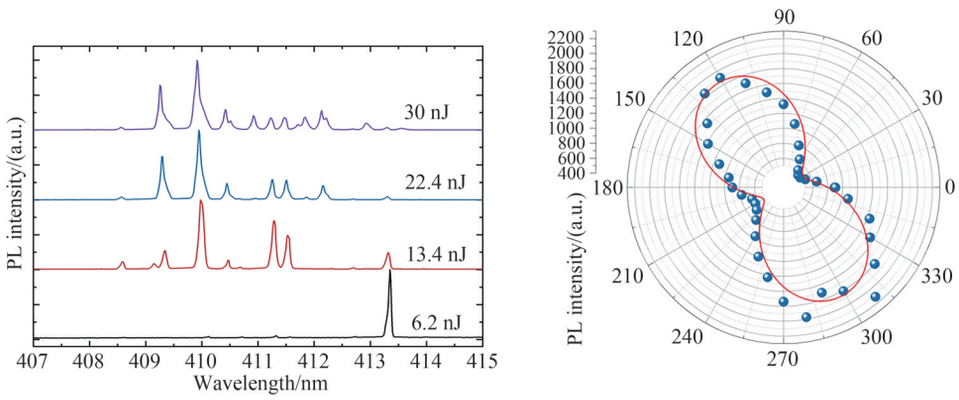

(a) High resolution normalized spectra under different excitation energy

(b) Polarization characteristic of the microdisk

图5 微盘器件模式与偏振特性

Fig.5 Mode and polarization characteristics of microdisk devices

除了阈值之外，Q值也是衡量GaN基微盘谐振腔性能优劣的一个重要的参数。Q值的定义为谐振腔内总存储能量除以光场在振荡周期2π弧度上的能量损失[40]。可通过谐振腔模式线宽进行计算

$$Q=\frac{\lambda}{\Delta\lambda} \tag{2}$$

式中，λ是模式中心波长，$\Delta\lambda$是模式半高宽。高Q值意味着更小的模式损耗、谐振腔内更长的光子寿命以及更好的时间相干性，可以促进腔内光与物质的相互作用。高Q值谐振腔也对窄线宽激光器至关重要，在相干光通信系统和光学测量系统中有着重要应用[41]。为了表征本工作中GaN微盘腔的Q值，测量了器件在阈值附近409 nm处谐振模式的高分辨率发光光谱，并对其进行了多峰洛伦兹拟合，如图6。可以看出模式半宽低至0.039 nm，已接近光谱仪最高分辨率（0.03 nm），计算得到谐振腔Q值为10 487。本文中GaN基微盘腔的高Q值主要归因于腔内极低的散射和吸收损耗。半导体微腔的Q值与其中各项损耗的关系可表示为

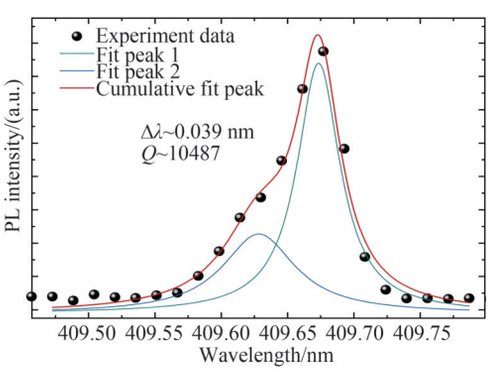

图6 微腔高分辨率发光光谱

Fig. 6 High resolution emission spectrum of the GaN based microcavity

$$Q^{-1}=Q_{th}^{-1}+Q_{abs}^{-1}+Q_{scat}^{-1} \tag{3}$$

式中，Q_{th}是从电磁理论所计算得出的Q值，Q_{abs}与谐振腔内部吸收损耗相关，Q_{scant}则与由表面以及侧壁粗糙度引起的散射损耗相关[41]。微盘侧壁的粗糙度难以准确测量，但是通过优化ICP蚀刻工艺，可以在器件制备中得到较为光滑的侧壁，如图3中SEM图所示。通过优化抛光工艺，微盘器件表面均方根粗糙度可以降低至0.4 nm以下，因此可极大降低器件的散射损耗。因此本工作中，限制Q值的主要因素是内部吸收损耗Q_{abs}，其可近似为

$$Q_{abs}^{-1}=\frac{\alpha\lambda}{2\pi n_{eff}} \tag{4}$$

式中，α为平均吸收系数，n_{eff}为介质的有效折射率，λ为所考虑模式的波长。在具有高缺陷/位错密度的GaN外延层中，由于带边和缺陷态之间的电子跃迁，其内部的吸收损耗非常显著[36]。NEYSHA L等通过光热偏

转光谱法研究了具有不同缺陷和位错密度的GaN外延层的吸收特性，发现其主要来源于靠近表面或靠近成核层的少部分区域[42]。此外，也有较多外延层中缺陷吸收主要来自高缺陷密度成核层的相关报道[43-44]。本文中，成核层以及其附近的高缺陷密度的外延层被去除，因此与直接在Si衬底上生长的微盘相比，可以实现更低的外延层平均吸收系数，进而实现更高的Q值。这种方法在传统的Si基GaN微盘谐振腔中是难以实现的。

在实际应用中，能够实现高温工作是光电器件一个重要的优势，为了探究器件在高温下的工作特性，在20 ℃～100 ℃范围内对器件进行了变温测试，其不同温度下阈值特性曲线如图7(a)。可以看出，器件在100 ℃仍能保持激射。随着温度增加，器件发光强度有所下降，但是激射阈值仅表现出小幅度增加。器件阈值随温度变化曲线如图7(b)。当环境温度从20 ℃增加至100 ℃时，相应阈值能量由5.2 nJ/pulse增加至10 nJ/pulse。这表明在器件在高温下仍有着良好的激射特性，主要归因于高质量的晶体材料与低损耗谐振腔的制备。

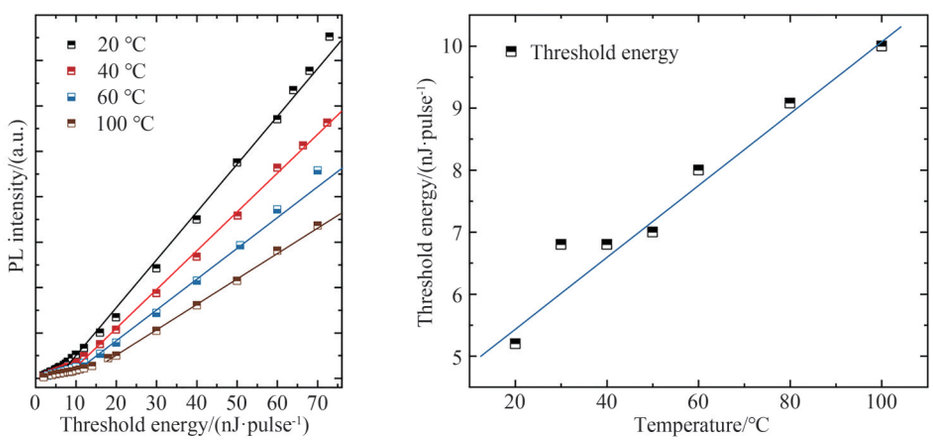

(a) Emission intensity as a function of excitation energy under different temperature

(b) Threshold energy as a function of environment temperature

图7 微盘器件变温激射特性

Fig.7 Ariable temperature maser characteristics of microdisk devices

3 结论

本文提出了一种在Si衬底上制备低阈值、高Q值GaN微谐振腔的新方法，避免了传统Si基GaN微腔中质量较差的外延层对器件的影响，在光泵浦条件下实现了高Q值的低阈值激射。阈值能量低至5.2 nJ/pulse，谐振腔Q值高达10 487。由于良好的晶体质量以及低损耗谐振腔，器件在100 ℃高温下仍能保持优异的激射特性。

参考文献

[1] ROLAND I, ZENG Y, CHECOURY X, et al. Near-infrared III-nitride-on-silicon nanophotonic platform with microdisk resonators[J]. Optics Express, 2016, 24(9): 9602-9610.

[2] WEISBUCH C, NISHIOKA, ISHIKAWA A, et al. Observation of the coupled exciton-photon mode splitting in a semiconductor quantum microcavity[J]. Physical Review Letters, 1992, 69(23): 3314-3317.

[3] FENG M, WANG J, ZHOU R, et al. On-chip integration of GaN-based laser, modulator, and photodetector grown on Si [J]. IEEE Journal of Selected Topics in Quantum Electronics, 2018, 24(6): 1-5.

[4] NAKAMURA S, MUKAI T, SENOH M. Candela-class high-brightness InGaN/AlGaN double-heterostructure blue-light-emitting diodes[J]. Applied Physics Letters, 1994, 64(13): 1687-1689.

[5] ATHANASIOU M, SMITH R, LIU B, et al. Room temperature continuous-wave green lasing from an InGaN microdisk on silicon[J]. Scientific Reports, 2014, 4(1): 1-5.

[6] HU H, TANG B, WAN H, et al. Boosted ultraviolet electroluminescence of InGaN/AlGaN quantum structures grown on high-index contrast patterned sapphire with silica array[J]. Nano Energy, 2020, 69: 104427.

[7] ZHAO X, TANG B, GONG L, et al. Rational construction of staggered InGaN quantum wells for efficient yellow light-emitting diodes[J]. Applied Physics Letters, 2021, 118(18): 182102.

[8] WU J, LONG H, SHI X, et al. Polariton lasing in InGaN quantum wells at room temperature [J]. Opto-Electronic

Advances, 2019, 2(12):190014.
[9] BHATTACHARYA A, BATEN M Z, IORSH I, et al. Room-temperature spin polariton diode laser[J]. Physical Review Letters, 2017, 119(6): 067701.
[10] KÖNIG H, ALI M, BERGBAUER W, et al. Visible GaN laser diodes: from lowest thresholds to highest power levels[C]. Novel In-Plane Semiconductor Lasers XVIII, 2019.
[11] GIL-SANTOS E, BAKER C, NGUYEN D T, et al. High-frequency nano-optomechanical disk resonators in liquids[J]. Nature Nanotechnology, 2015, 10(9): 810-816.
[12] VAHALA K J. Optical microcavities: Photonic technologies[J]. Nature, 2003, 424: 839-846.
[13] YANG K, HAO Y Z, WU J L, et al. Mode characteristics for gapless-coupled twin circular-side square microcavity lasers[J]. Journal of the Optical Society of America B, 2021, 38(3): 1017-1023.
[14] AKASAKI I, AMANO H, KOIDE Y, et al. Effects of ain buffer layer on crystallographic structure and on electrical and optical properties of GaN and Ga1-xAlxN ($0<x\leqq 0.4$) films grown on sapphire substrate by MOVPE[J]. Journal of Crystal Growth, 1989, 98(1-2): 209-219.
[15] MURASE T, TANIKAWA T, HONDA Y, et al. Optical properties of (1-101) InGaN/GaN MQW stripe laser structure on Si substrate[J]. Physica Status Solidi C, 2011, 8(78): 2160-2162.
[16] ZHANG Y, ZHANG X, LI K H, et al. Advances in III-nitride semiconductor microdisk lasers[J]. Physica Status Solidi A, 2015, 212(5): 960-973.
[17] HAN X, LIU Y, REN Y, et al. Semipolar {1 122} InGaN/GaN multiple quantum well optically pumped laser diodes selectively grown on Si (111) substrates[J]. Materials Science in Semiconductor Processing, 2019, 91: 327-332.
[18] SUN Y, ZHOU K, QIAN S, et al. Room-temperature continuous-wave electrically injected InGaN-based laser directly grown on Si[J]. Nature Photonics, 2016, 10(9): 595-599.
[19] TANG Y, FENG M, WEN P, et al. Degradation study of InGaN-based laser diodes grown on Si[J]. Journal of Physics D: Applied Physics, 2020, 53(39): 395103.
[20] FENG M, LI Z, WANG J, et al. Room-temperature electrically injected AlGaN-based near-ultraviolet laser grown on Si[J]. Acs Photonics, 2018, 5(3): 699-704.
[21] TAMBOLI A C, HABERER E D, SHARMA R, et al. Room-temperature continuous-wave lasing in GaN/InGaN microdisks[J]. Nature photonics, 2007, 1(1): 61-64.
[22] ZHANG Y, MA Z, ZHANG X, et al. Optically pumped whispering-gallery mode lasing from 2-μm GaN micro-disks pivoted on Si[J]. Applied Physics Letters, 2014, 104(22): 221106.
[23] ZHU G Y, QIN F F, GUO J Y, et al. Unidirectional ultraviolet whispering gallery mode lasing from floating asymmetric circle GaN microdisk[J]. Applied Physics Letters, 2017, 111(20): 202103.
[24] LI D, GAO H, WANG H, et al. Room-temperature electrically pumped InGaN-based microdisk laser grown on Si[J]. Optics Express, 2018, 26(4): 5043-5051.
[25] WANG J, FENG M, ZHOU R, et al. Continuous-wave electrically injected GaN-on-Si microdisk laser diodes[J]. Optics Express, 2020, 28(8): 12201-12208.
[26] AHARONOVICH I, WOOLF A, RUSSELL K J, et al. Low threshold, room-temperature microdisk lasers in the blue spectral range[J]. Applied Physics Letters, 2013, 103(2): 021112.
[27] SELLES J, BRIMONT C, CASSABOIS G, et al. Deep-UV nitride-on-silicon microdisk lasers[J]. Scientific Reports, 2016, 6(1): 1-7.
[28] SELLES J, CREPEL V, ROLAND I, et al. III-Nitride-on-silicon microdisk lasers from the blue to the deep ultra-violet[J]. Applied Physics Letters, 2016, 109(23): 231101.
[29] ZHAO C, TANG C W, WANG J, et al. Ultra-low threshold green InGaN quantum dot microdisk lasers grown on silicon[J]. Applied Physics Letters, 2020, 117(3): 31104.
[30] DADGAR A, STRITTMATTER A, BLÄSING J, et al. Metalorganic chemical vapor phase epitaxy of gallium-nitride on silicon[J]. Physica Status Solidi, 2010(6): 1583-1606.
[31] DADGAR A, SCHULZE F, ZETTLER T, et al. In situ measurements of strains and stresses in GaN heteroepitaxy and its impact on growth temperature[J]. Journal of Crystal Growth, 2004, 272(1/4): 72-75.
[32] SUN Q, YAN W, FENG M, et al. GaN-on-Si blue/white LEDs: epitaxy, chip, and package[J]. Journal of Semiconductors, 2016, 37(4): 044006.
[33] WANG J, FENG M, ZHOU R, et al. Continuous-wave electrically injected GaN-on-Si microdisk laser diodes[J]. Optics express, 2020, 28(8): 12201-12208.
[34] SUN Y, ZHOU K, SUN Q, et al. Room-temperature continuous-wave electrically injected InGaN-based laser directly grown on Si[J]. Nature Photonics, 2016, 10(9): 595-599.
[35] BUTTÉ R, GRANDJEAN N. III-nitride photonic cavities[J]. Nanophotonics, 2020, 9(3): 569-598.
[36] PUCHTLER T J, WOOLF A, ZHU T, et al. Effect of threading dislocations on the quality factor of InGaN/GaN

microdisk cavities[J]. Acs Photonics, 2015, 2(1): 137-143.
[37] MEI Y, XIE M, XU H, et al. Electrically injected GaN-based microdisk towards an efficient whispering gallery mode laser[J]. Optics Express, 2021, 29(4): 5598-5606.
[38] WANG D, ZHU T, OLIVER R A, et al. Ultra-low-threshold InGaN/GaN quantum dot micro-ring lasers[J]. Optics Letters, 2018, 43(4): 799-802.
[39] TABATABA-VAKILI F, BRIMONT C, ALLOING B, et al. Analysis of low-threshold optically pumped III-nitride microdisk lasers[J]. Applied Physics Letters, 2020, 117(12): 121103.
[40] GAČEVIĆ Ž, ROSSBACH G, BUTTÉ R, et al. Q-factor of (In, Ga) N containing III-nitride microcavity grown by multiple deposition techniques[J]. Journal of Applied Physics, 2013, 114(23): 233102.
[41] ROUSSEAU I, CALLSEN G, JACOPIN G, et al. Optical absorption and oxygen passivation of surface states in III-nitride photonic devices[J]. Journal of Applied Physics, 2018, 123(11): 113103.
[42] LOBO N, KADIR A, LASKAR M R, et al. Influence of growth parameters on the sub-bandgap absorption of MOVPE-grown GaN measured using photothermal deflection spectroscopy[J]. Journal of Crystal Growth, 2008, 310(23): 4747-4750.
[43] MIERRY P D, LAHRECHE H, HAFFOUZ S, et al. Sub-bandgap optical absorption of MOVPE-GaN grown under controlled nucleation[J]. Materials Science and Engineering: B, 1999, 59(1-3): 24-28.
[44] SCHAD S S, NEUBERT B, EICHLER C, et al. Absorption and light scattering in InGaN-on-sapphire-and AlGaInP-based light-emitting diodes[J]. Journal of Lightwave Technology, 2004, 22(10): 2323-2332.

Fabrication and Lasing Properties of Silicon-based GaN Microcavities(Invited)

MA Lilong, XIE Minchao, OU Wei, MEI Yang, ZHANG Baoping
(*Laboratory of Micro/Nano-Optoelectronics*, *School of Electronic Science and Engineering*, *Xiamen University*, *Xiamen*, *Fujian* 361005, *China*)

Abstract: Semiconductor microcavities can restrict photons in a small volume compared to the wavelength of light, and can artificially adjust the spontaneous emission characteristics of the active medium in the cavity, which is important for the development of more efficient optoelectronic devices. At the same time, semiconductor microcavities also provide a good platform for the fundamental research of cavity quantum electrodynamics. Optoelectronic devices based on semiconductor microcavity have been widely used, such as microcavity lasers, microcavity sensors, microcavity optical filters, etc. Optical microcavities are usually divided into three types: Fabry-Pérot (FP) microcavities, Photonic Crystal (PC) microcavities, and Whispering-gallery Mode (WGM) microcavities. In WGM semiconductor microcavities, photons circulate along the sidewall of the waveguide layer, and the optical field is confined by total reflection at the interface between the waveguide layer and the surrounding air. Therefore, WGM microcavities can achieve high quality (Q) value and small mode volume. Compared with the FP and PC microcavities, WGM microcavities have the advantages of simple structure, convenient preparation, and easy integration with large scale optoelectronic circuits. GaN based semiconductor materials are featured with direct wide bandgap, including aluminum nitride, gallium nitride, indium nitride, and a variety of alloys between them. By adjusting the composition of the alloy, the emission wavelength can cover from deep ultraviolet to the near-infrared band. They are very important for the preparation of optoelectronic devices. In addition, GaN based semiconductor materials with high exciton binding energy and oscillator strength can be combined with WGM microcavity to achieve micro-cavity optoelectronic devices with small size and high efficient, which can be used for cavity quantum electrodynamics studies at room temperature. Therefore, GaN-based WGM microcavity light-emitting devices have attracted the attention of many researchers, and have been widely used in optoelectronic integration, spectral analysis, and other fields.

To date, there have been many reports about GaN microdisk based lasers and sensors on Si, and laser emission wavelengths have covered from UVC to the green spectral range. However, GaN based microdisk cavities on Si are also faced with many difficulties, including the lattice constant mismatch and thermal expansion coefficient mismatch between GaN and Si substrates, and the melt etching during epitaxial growth, etc. There is a 17% lattice mismatch between GaN and silicon, usually resulting in a high

threading dislocation density (typically 1 010 cm^{-2}) during epitaxial growth. This can reduce the internal quantum efficiency of the active region, and cause the interface roughness of the GaN film, thus increasing the scattering loss of the microcavity. On the other hand, the thermal expansion coefficient mismatch between GaN and Si substrate is as large as 54%, which leads to large tensile stress in GaN film during the cooling process after epitaxial growth, resulting in wafer warping and even cracking. Therefore, to ensure the quality of the active region, it is usually necessary to grow thick stress adjustment and defect filtration layers. Moreover, the Ga source used in epitaxial growth can corrode Si substrate, that is, melt etching. A certain thickness of AlN buffer layer is usually grown to protect Si substrate before GaN growth. As a result, the total thickness of GaN epitaxial layer on Si substrate is large (generally >1 μm). The large thickness of microdisk makes it difficult to guarantee the single-mode operation, and can reduce the light confinement ability and microcavity effect. In addition, the nitrides near the substrate often have high density defects and dislocations, and their internal optical absorption and scattering losses can be large. This can also affect the *Q* factor and the threshold of the microdisk laser.

To solve the above problems, a new method of device preparation is proposed in this study. Devices fabricated by this method avoid the influence of poor crystal quality and large thickness of GaN layers directly grown on Si substrate. Sapphire substrate is used for the GaN growth in this study to ensure crystal quality. During the fabrication of microdisks, the epitaxial layer was transferred to the Si substrate, and the rich defect layer close to the substrate during the original growth was removed. After that, a simple SiO_2 sacrificial layer wet etching technique was used to realize the air gap structure between GaN microdisk and Si. High *Q* GaN microdisk cavity on Si with low lasing threshold was successfully realized under the condition of optical pumping. The cavity *Q* factor is up to 10 487. The device threshold energy is as low as 5.2 nJ/pulse, corresponding to an energy density of 33.6 $\mu J/cm^2$. Owing to the good crystal quality and low cavity losses, the device can still maintain excellent laser characteristics at 100 ℃. The device preparation method in this study also has good flexibility, and the GaN-based microdisk resonator can be fabricated on different kinds of substrates, such as metal, polymer, quartz, etc.

Key words: Semiconductor devices and technology; Microcavity; GaN; Si; High *Q* factor; Low threshold; High temperature operation

OCIS Codes: 140.3945; 140.3540; 160.4760; 160.6000

Foundation item: National Key Research and Development Program of China (No. 2017YFE0131500), National Natural Science Foundation of China (No. 62104204), President's Foundation of Xiamen University (No. ZK1029)